applied sciences

MDPI

Article

The Analysis of Stiffness and Driving Stability in Cross-Member Reinforcements Based on the Curvature of a Small SUV Rear Torsion Beam Suspension System

Keunuk Chung [1], Yeonghoon Lee [1] and Jinwook Lee [2,*]

[1] School of Mechanical Engineering, Undergraduate Course, Soongsil University, Seoul 06978, Republic of Korea; gju05225@gmail.com (K.C.); lyh8690@naver.com (Y.L.)
[2] School of Mechanical Engineering, Soongsil University, Seoul 06978, Republic of Korea
* Correspondence: immanuel@ssu.ac.kr; Tel.: +82-2-820-0929

Abstract: Most small SUVs in the automotive market are equipped with torsion beam suspension for the rear wheels. Torsion beam suspension consists of a cross-member and a trailing arm. The cross-member plays a crucial role in preventing the vehicle from twisting; therefore, a shape that can withstand loads is essential. In this study, various shapes of cross-member reinforcements were added to the existing torsion beam suspension to analyze its structural strength when subjected to arbitrary forces. Analysis results were obtained for stiffness and driving stability factors such as smooth road shake, impact hardness, and memory shake. Based on these results, we identified the optimal cross-member shape with low torsional stiffness and a small side view swing arm angle by examining the changes in driving stability.

Keywords: torsion beam suspension; stiffener curvature; bending stress; torsional stress; torsional rigidity; cross-member; side view swing arm angle; smooth road shake; impact hardness; memory shake

check for updates

Citation: Chung, K.; Lee, Y.; Lee, J. The Analysis of Stiffness and Driving Stability in Cross-Member Reinforcements Based on the Curvature of a Small SUV Rear Torsion Beam Suspension System. *Appl. Sci.* **2023**, *13*, 12067. https://doi.org/10.3390/app132112067

Academic Editor: Giangiacomo Minak

Received: 20 September 2023
Revised: 29 October 2023
Accepted: 30 October 2023
Published: 6 November 2023

1. Introduction

1.1. Background of the Study

Owing to recent increases in fuel prices and economic downturn, consumers are increasingly looking for reasonably priced and cost-effective options. The sales of small SUVs with sufficient trunk space and capacity to accommodate two or more passengers have been on the rise. According to the Korea Automobile Manufacturers Association, one vehicle model from Company H recorded approximately 6000 units in sales in March 2023, which marks an increase of approximately 3000 units over the previous month [1]. In Asian countries such as Japan and China, small SUVs rank high in total sales. Recently, with the tightening of carbon dioxide emission regulations in Europe, the negative perception of conventional small SUVs has shifted in a positive direction.

The demand and sales of small SUVs have been on the rise owing to the alignment of environmental regulations and high fuel prices. Most SUVs use the torsional beam suspension as their rear suspension system. A torsional beam suspension is an integral type of suspension in which a single torsion beam is connected to the trailing arms to support each wheel. Therefore, the torsion beam suspension is expected to have inferior vibration absorption capabilities for each wheel compared to independent rear suspension systems. Thus, the issue of ride comfort dissatisfaction remains unresolved.

Kang [2,3] conducted a geometric analysis of key suspension design factors such as roll steer and roll camber for the torsion beam suspension and suggested that to optimize the reinforcement design to increase roll stiffness, it is necessary to calculate the warping of the torsion beam cross-section. Kim et al. [4] employed experimental design methods to design the torsion beam cross-section and minimize the beam thickness, resulting in an approximately 8% reduction in weight. Jang et al. [5] achieved improved stiffness, durability, and a weight reduction of 3.5 kg by utilizing a tubular-shaped torsion beam, instead of the plate-shaped torsion beam used by the aforementioned researchers, and adopting the hot stamping method instead of the conventional hydroforming method. Lee et al. [6] changed the torsion beam material to high-strength steel and conducted stress analysis experimentally. Choi et al. [7] studied durability by employing different torsion beam shape models and conducting structural and fatigue analyses. Lee et al. [8] observed that increasing the stiffness of the components in the torsion beam suspension induced vibration phenomena at high speeds and improved the ride comfort perceived by the driver.

Zhang et al. [9] compared equivalent spring modeling methods with MNF flexible body modeling methods and found that the modified beam modeling method showed the highest simulation accuracy. Gao et al. [10] investigated the impact of the busing installation angle and bushing stiffness of the torsion beam suspension on the overall vehicle performance. They determined that the vehicle exhibited the best understeer characteristics and optimal steady-state performance when the bushing installation angle was near $-22.5°$. After optimization, they concluded that significant improvements in vehicle performance were achieved with a bushing installation angle of $-27.7°$. Ren et al. [11] conducted a strength analysis of torsion beam suspension for an MPV vehicle. They utilized ADAMS to model the torsion beam suspension and reported the maximum stresses applied to the beam in various conditions: 529.5 MPa in bumpy conditions, 238.8 MPa while braking, 168.8 MPa while accelerating, and 335.9 MPa while steering. Taking these stresses into account, they emphasized the importance of selecting the appropriate material and thickness for the cross-member. Wang et al. [12] investigated the maximum stresses applied not only to the beam in the torsion beam suspension but also to the brackets and reinforcing plate integrated into the trailing arm. Jeong et al. [13] performed shape optimization of the torsion beam to create an H-shaped torsion beam model. This resulted in an understeer gradient that was 3.07% greater than the base model, and the response and peak times of the lateral acceleration were 8% and 6.25% lower than the base model, respectively. Through this, they validated the improvement in the dynamic response performance of the optimized vehicle. In other studies, better ride comfort performance was reported when an active suspension was used [14], and it was found that increased suspension charging pressure led to higher vibrations [15]. Ali [16] developed a quantitative ride comfort index called AR by linearizing a nonlinear passenger mode. Donghui et al. [17] analyzed ride comfort according to age group and reported that at speeds of 30–70 km/h, child seats encounter greater acceleration, resulting in reduced comfort. Kobayashi et al. [18] analyzed ride comfort according to posture; anthropometric accuracy was studied using a sitting human model through lumped parameters with 4 degrees of freedom. Jung et al. [19] conducted research on improving regenerative braking efficiency in electric vehicles.

Previous studies have investigated the ride comfort of vehicles equipped with torsion beam suspension using various variables. However, no prior study has conducted a stiffness analysis by adding different shapes of cross-member reinforcements to the torsion beam.

1.2. Research Objective

This study aimed to enhance the structural stability of torsion beam suspension for the rear wheels of small SUVs. The objective was to maintain the existing torsion beam suspension shape while improving its stability through modifications to the cross-member reinforcement shape. Based on previous research findings [3], the existing parameters were retained, and cross-member reinforcements were added to the torsion beam suspension to analyze their effects. Using SolidWorks, six different cross-sectional shapes and one reference shape were modeled based on the overall structure of the torsion beam [4]. Material selection for the modeling was carried out, and a stiffness analysis was conducted to examine the stress and stiffness when applying loads to the endpoints of the beam, while considering vehicle rotation.

This study investigated cross-member shapes that offer driving stability advantages by examining the influence of curvature variation in cross-member reinforcements on the torsion beam suspension. Factors associated with driving stability, smooth road shake (SRS), impact hardness, and memory shake were applied to assess the vibrations transmitted through the torsion beam suspension.

SRS refers to the vibrations transmitted to the seat and foot floor panel by unbalanced masses in specific speed ranges. These unbalanced masses induce vertical, yaw, and camber movements through the torsion beam suspension, resulting in a negative riding stability for the driver [8]. Impact hardness refers to longitudinal and vertical accelerations when a vehicle experiences sudden impacts. Memory shake refers to the vibrations transmitted to the driver in the vertical and longitudinal directions for a certain period after impact. Although impact hardness and memory shake exhibit contrasting characteristics, when considering memory shake as a reference, they do not necessarily show opposing features [20]. To understand these three quality factors, the side view swing arm (SVSA) angle was used as a key parameter. The SVSA angle is a significant geometric factor that affects the ride comfort performance of a vehicle; a negative SVSA angle indicates superior ride comfort [8].

This study selected a stable torsional stiffness and optimized the SVSA angle according to the cross-member section with different curvature reinforcements. Figure 1 shows the overall analysis of this study.

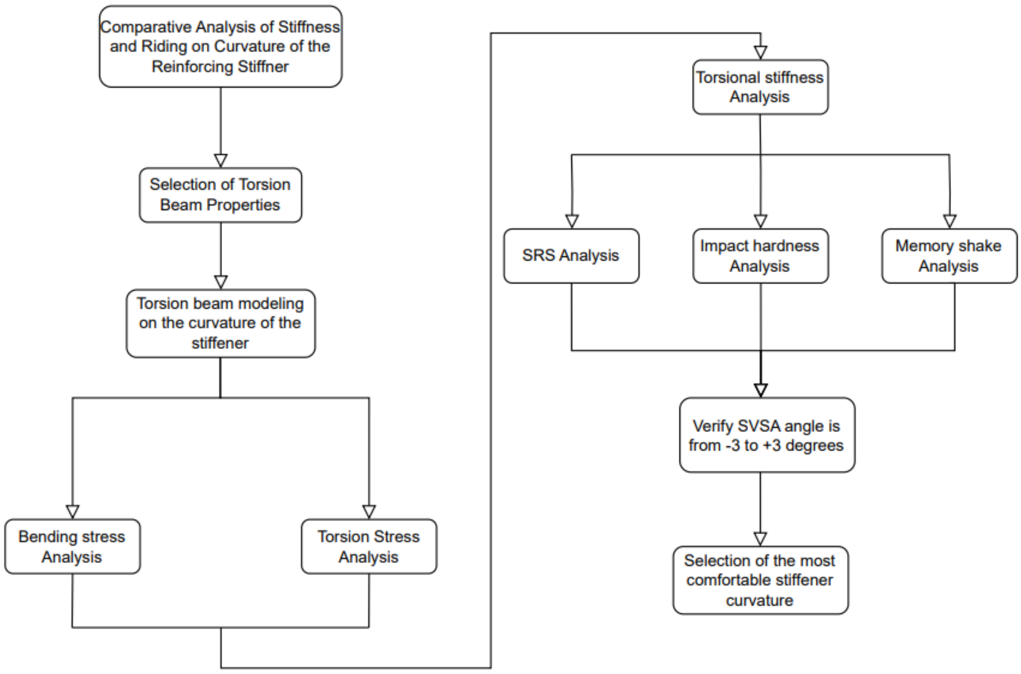

Figure 1. Flow chart of the analysis process followed in this study.

2. Research Methods

2.1. Torsion Beam Shape and Properties

Figure 2 shows the location of the torsion beam suspension as a rear suspension system in a small SUV, and Figure 3 shows the structure of the torsion beam suspension. The torsion beam is positioned between the left and right trailing arms. A torsion beam typically features a V-shaped open cross-sectional design to facilitate torsional movement. When the vehicle rotates to the left or right, a rolling motion occurs, and the torsion beam can be deformed due to the torsional stress. The torsional stiffness of the torsion beam significantly influences the roll stiffness of the vehicle. Appropriate material selection is crucial for analyzing torsional stiffness. Given the welding configuration between the torsion beam and the trailing arms, a weldable material is desirable. Based on relevant research [21], SAPH440 was selected for the torsion beam. The mechanical properties of the torsion beams are listed in Table 1.

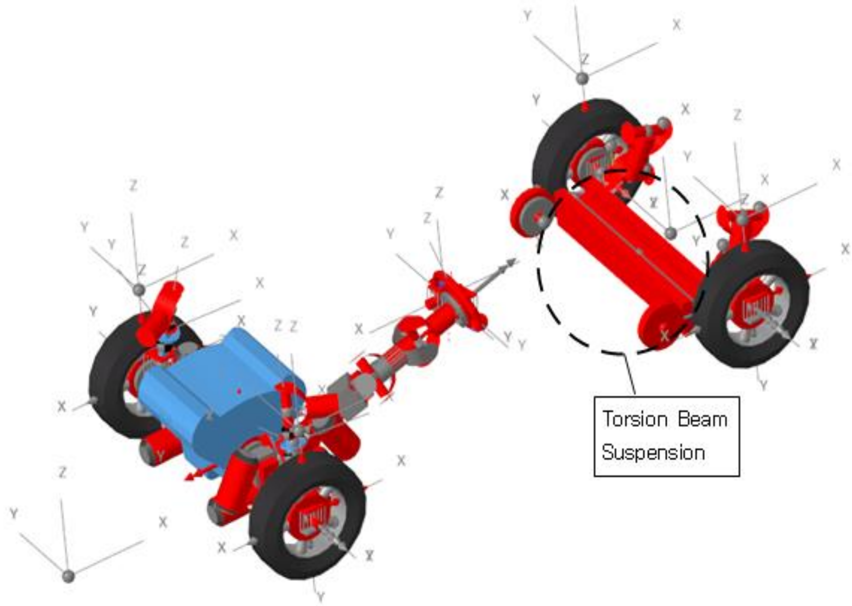

Figure 2. Location of torsion beam.

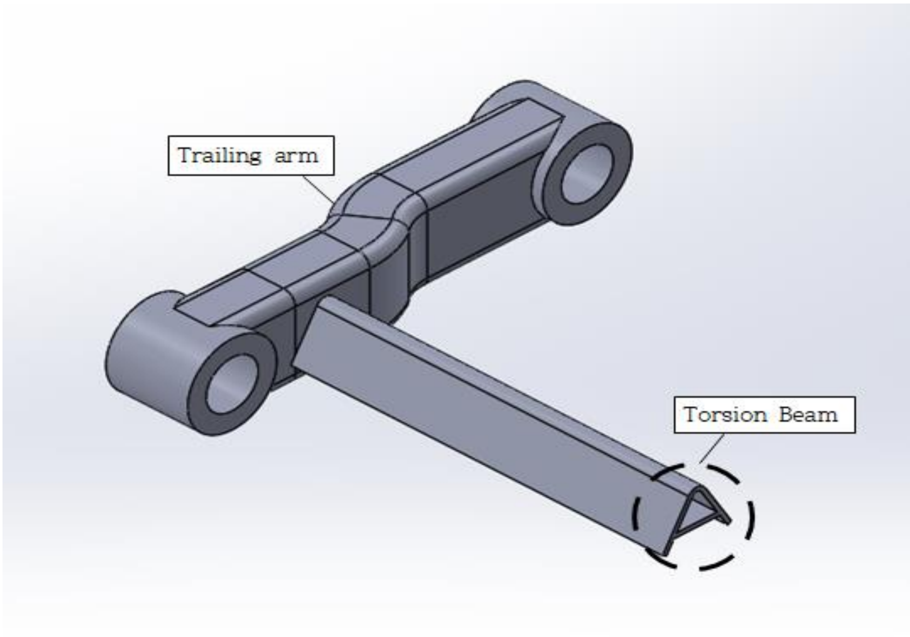

Figure 3. Overall structure of torsion beam.

Table 1. SAPH440 material properties.

Property	Unit	Value
Young's modulus	GPa	207
Poisson's ratio	-	0.3
Mass density	kg/m^3	7810
Tensile strength	MPa	440
Yield strength	MPa	300

2.2. Torsion Beam Modeling

The shape of the torsion beam was modeled based on the results obtained by Kang [3]. The analysis model of the torsion beam was created using SolidWorks, and before the shape design, the left and right sides of the beam were merged into a single point for modeling.

The essential parameters of this model are shown in Figure 4. The thickness was fixed at 6 t, with an L of 70 mm, the curvature radius R of 10 mm, and an angle of 60 degrees. The reinforcement position, M, was set to 24 mm. These parameter values are detailed in Table 2. Using the above basic parametric values, the reinforcement was based on a straight line, and it was bent up and down, designed, and compared.

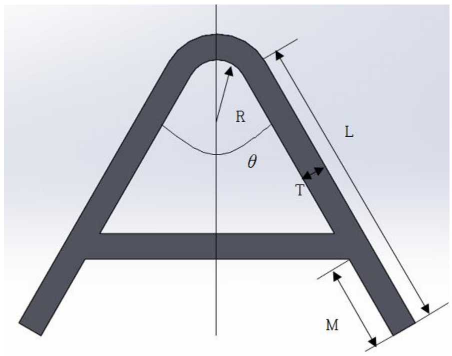

Figure 4. Parameters of cross-member.

Table 2. Modeling parameters used in this study.

Parameter	Unit	Value
T	Mm	6
L	Mm	70
R	Mm	10
θ	°(deg)	60
M	Mm	24
Torsion beam Length	Mm	1200

Figure 5 shows the cross-sectional shapes modeled in this study. The base configuration represents a torsion beam with a straight reinforcement and serves as a reference for the analysis. The Type 1, Type 2, and Type 3 configurations had upward convex reinforcements, denoted by a "+" sign, and their curvature radii were +40 mm, +50 mm, and +60 mm, respectively. The Type 4, Type 5, and Type 6 configurations had downward concave reinforcements, denoted with a "−" sign, and their curvature radii were −40 mm, −50 mm, and −60 mm, respectively.

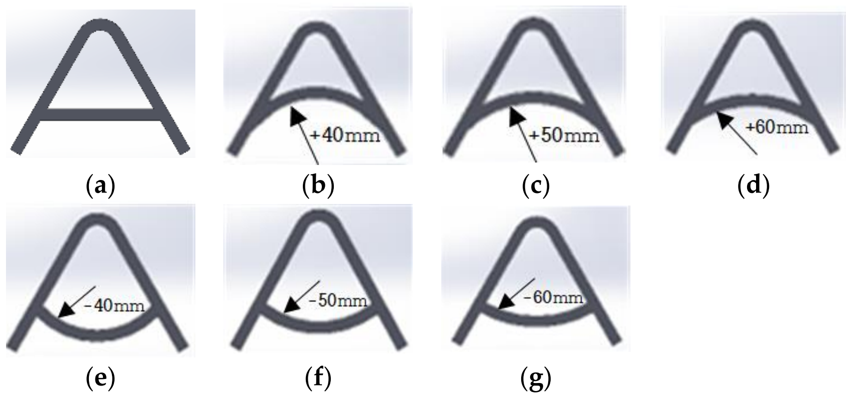

Figure 5. Cross-member shapes investigated in this study. (**a**) Base; (**b**) Type 1; (**c**) Type 2; (**d**) Type 3; (**e**) Type 4; (**f**) Type 5; (**g**) Type 6.

2.3. 3D Model of the Cross-Sectional Shape for Structural and Rigidity Analysis

To analyze the structure and stiffness of the torsion beam suspension, it was necessary to first create a 3D model of the cross-sectional shapes shown in Figure 5. To achieve this, the wheelbase of Company H's small SUV was used as a reference, and the horizontal length was set to 1200 mm [22].

Meshes were generated for each model to analyze the bending stress using SolidWorks. For the rotational analysis of the vehicle, one side was fixed, and an arbitrary load of 2000 N was applied to the opposite side. Similarly, for the shear stress analysis, meshes were created and an arbitrary torsional load of 2000 N was applied while fixing one side.

The torsional stiffness was calculated using the following equation:

$$\text{Torsional rigidity} = \frac{L * F}{\theta} \tag{1}$$

$$\theta = \tan^{-1}\left(\frac{\overline{y}}{L}\right) \tag{2}$$

Under the assumption that the force is applied downward, F represents the load, L is the total length in the horizontal direction, y represents the deflection in the y-axis due to the applied load, and theta represents the angular displacement. We used SolidWorks to determine the deflection under the load and calculated the torsional stiffness using Equations (1) and (2).

Figure 6 shows the results of the bending stress, torsional stress, and deflection along the y-axis for the base cross-member. The load was applied to the right side while keeping the left side fixed. The stress distribution revealed the locations where the load was the most significant.

2.4. Vehicle Model with the Baseline Cross-Member

The geometry of the torsion beam model is based on the specifications of Company H's 1600 cc small SUV with reference to Table 3. A vehicle model, with the baseline configuration as the foundation, is shown in Figure 7.

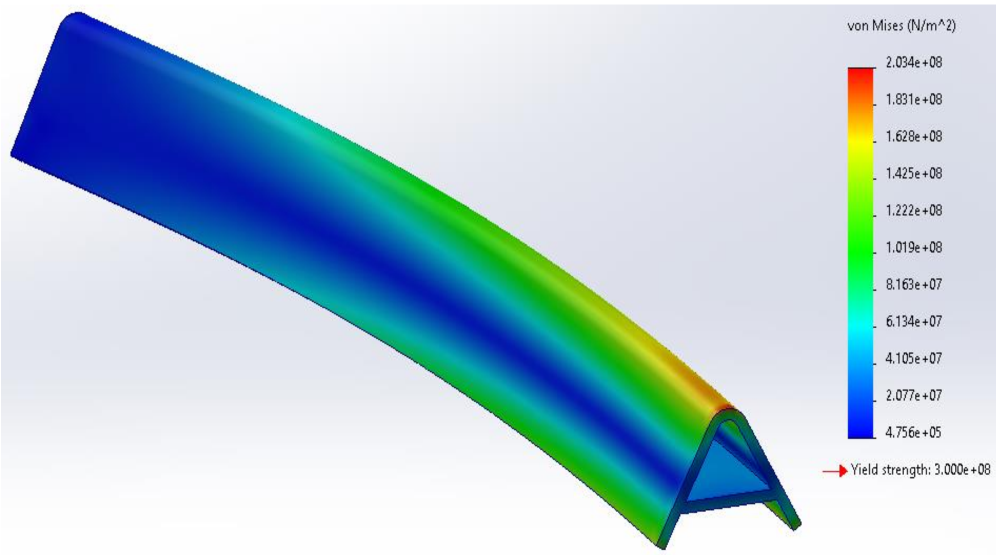

(**a**)

Figure 6. *Cont.*

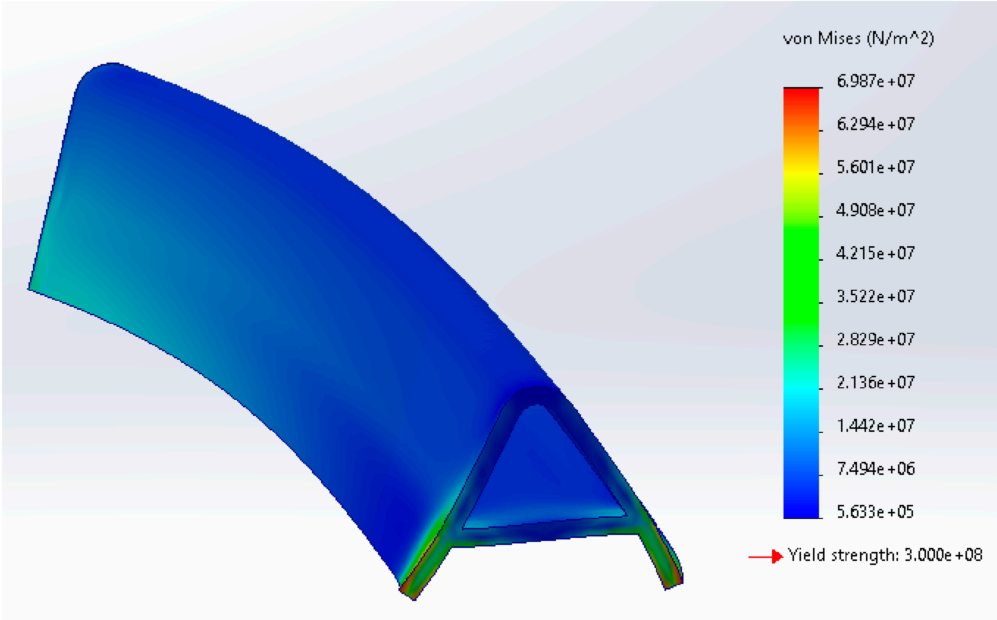

(**b**)

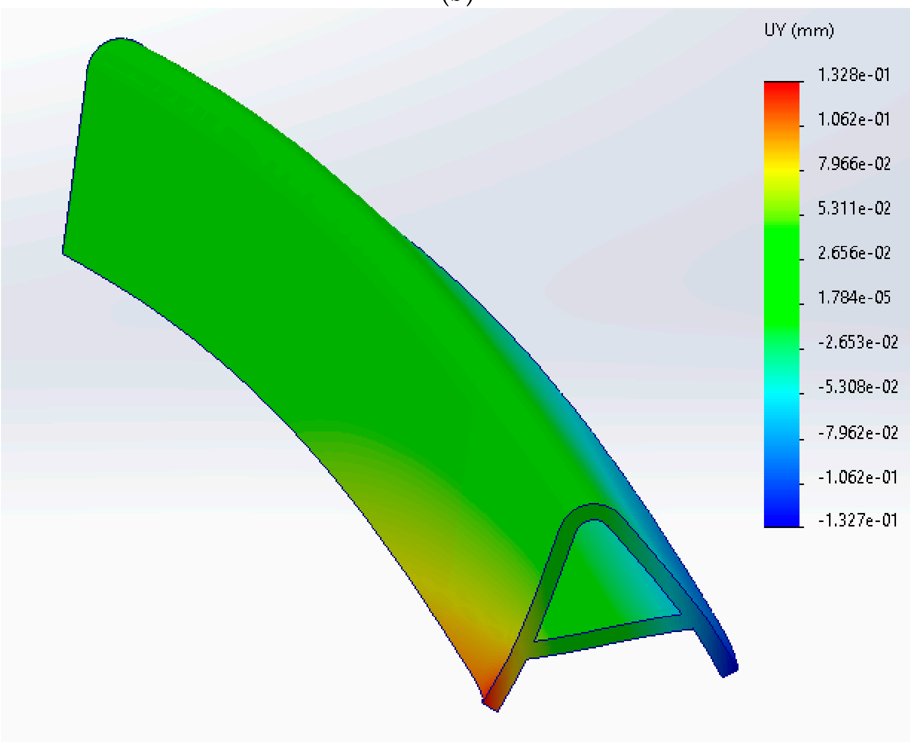

(**c**)

Figure 6. Analysis results for baseline cross-member (Base, in Figure 5a). (**a**) Bending stress; (**b**) torsional stress; (**c**) Y-axis displacement.

Table 3. Vehicle specifications considered in this study.

Item	Unit	Value
Wheel base	mm	2660
Front/Rear thread	mm	1590/1600
Drive method	-	FF
Front wheel suspension	-	MacPherson strut
Rear wheel suspension	-	Torsion beam

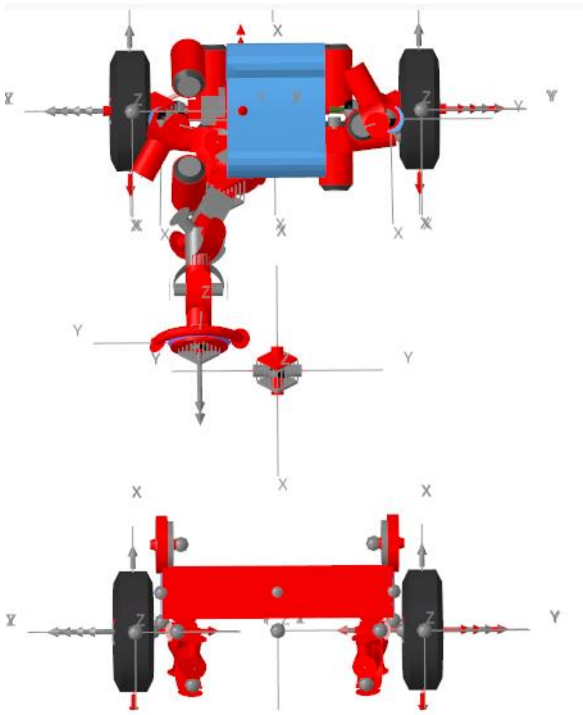

Figure 7. Vehicle model with the baseline cross-member configuration as the foundation.

2.5. Rear Torsion Beam Suspension Modeling

In this study, Altair MotionView was used as the preprocessing tool for the driving stability analysis, and numerical analysis was performed using Altair MotionSolve, which is based on multibody dynamics. The modeling used for the analysis included the front-wheel drive and shock absorbers; however, for simplification, only the rear-wheel torsion beam suspension was applied (Figure 8), excluding the front-wheel suspension, subframe, and stabilizer. The cross-sectional area and sectional moment of inertia were calculated for each configuration from Base to Type 6, and were incorporated into the model along with the material properties of SAPH 400. The Base type torsion beam properties can be found in Table 4. The vehicle parameters in this study reflecting the rear torsion beam suspension can be found in Table 5. The analysis was conducted for each configuration for 10 s. For scenarios involving driving on a flat road, static ride analysis was used, whereas for situations involving cornering and roll motions, static roll analysis was used to evaluate the ride comfort factors. The SVSA angle range was set from −3 degrees to +3 degrees to analyze whether the designed torsion beam configurations fell within the specified range.

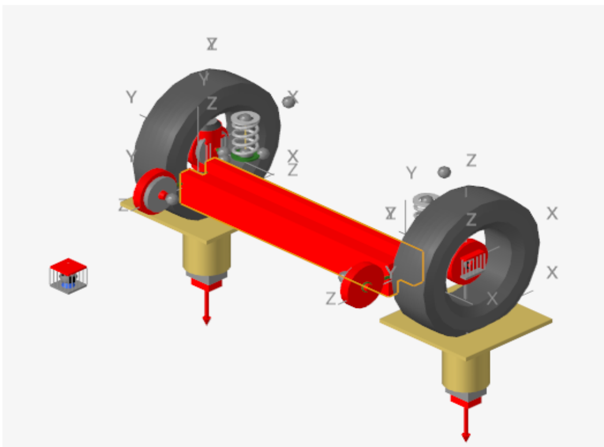

Figure 8. Rear torsion beam suspension.

Table 4. Base torsion beam properties.

Property	Unit	Value
Area	mm^2	1331.41
I_xx	mm^4	446,043.86
I_yy	mm^4	765,051.83
I_zz	mm^4	1,211,095.69

Table 5. Vehicle parameters considered in this study.

Parameter	Unit	Value
Vehicle end	-	Rear
Type	-	Dependent
Tire static loaded radius	Mm	310
Tire vertical spring rate	N/mm	350
CG height	Mm	795
Wheel base	Mm	2660
Vehicle weight	N	14,000
Front braking ratio	-	0.7
Front drive ratio	-	1.0
Axle ratio	-	3.0
Wheel travel in roll and ride	Mm	30

3. Results and Discussion

3.1. Bending and Torsional Stress Analysis

Table 6 presents the analysis results of the bending and torsional stresses for each torsional beam configuration. The stresses vary depending on the shape of the reinforcement. Among the convex shapes, Type 1, with a curvature of +40 mm, showed higher stresses than those of the baseline configuration (Base). As the curvature increased, the stresses decreased, but there was no significant difference compared with the baseline configuration.

Table 6. Results of bending and torsional stress.

Type	Stiffener Curvature (mm)	Bending Stress (MPa)	Torsional Stress (MPa)
Base	0	203.4	70.48
Type 1	+40	208.4	71.02
Type 2	+50	192.8	64.14
Type 3	+60	194.6	69.80
Type 4	−40	164.9	68.76
Type 5	−50	174.2	66.45
Type 6	−60	177.8	66.52

In contrast, for the concave shapes with added reinforcements (Types 4, 5, and 6), the stresses were lower than those of the base configuration. The torsional stress did not show significant variations with curvature, whereas the bending stress decreased as the curvature decreased. A lower bending stress indicates that the torsional beam can withstand the applied load with less deformation and is considered more stable under a load. Similarly, a lower torsional stress indicates that the torsion beam is less affected by twisting forces. Therefore, among all the configurations, the concave shape with added reinforcements exhibited the most stable performance. Specifically, the Type 4 configuration with the lowest bending stress was identified as the most stable structure.

3.2. Torsional Stiffness Analysis

Table 7 presents the torsional stiffness analysis results for each torsion beam configuration. Torsional stiffness refers to the structural rigidity of a beam subjected to torsional deformation; higher torsional stiffness implies reduced deformation under torsional loading.

Table 7. Torsional rigidity results.

Type	Stiffener Curvature (mm)	Y-axis Displacement (mm)	Angle (°)	Torsional Rigidity (N·m/deg)
Base	0	0.133	0.082	1124.7
Type 1	+40	0.229	0.142	651.8
Type 2	+50	0.193	0.119	777.8
Type 3	+60	0.178	0.110	841.5
Type 4	−40	0.0568	0.057	1629.5
Type 5	−50	0.0996	0.062	1500.2
Type 6	−60	0.105	0.065	1435.0

Based on the analysis results for Types 1, 2, and 3, which had convex-shaped reinforcements, the y-axis displacements were greater than those of the baseline configuration. The torsional stiffness of these configurations was lower than that of the baseline configuration, and as the curvature increased from +40 mm to +60 mm, the torsional stiffness increased.

In contrast, for Types 4, 5, and 6, which had concave-shaped reinforcements, all the configurations exhibited smaller y-axis displacements than the baseline configuration. The torsional stiffness of these configurations was higher than that of the baseline configuration, and as the curvature decreased from −60 mm, the torsional stiffness increased.

Based on these results, we can conclude that, among all the configurations, the concave-shaped reinforcements with higher torsional stiffness are less affected by torsional forces than the convex-shaped reinforcements. Among the concave-shaped configurations, Type 4, which had the highest torsional stiffness, was the most stable when subjected to torsional loading.

3.3. Driving Stability Analysis Based on SRS

As a factor associated with driving stability, smooth road shake (SRS) is generated by the unbalanced mass that occurs during the assembly and manufacturing of components such as tires and wheels. This is represented by the response of the acceleration transmitted to the foot floor panel during vehicle operation.

In this study, we analyzed the characteristics of the SRS response by varying the side view swing arm (SVSA) angle according to its sensitivity. To achieve this, we applied an unbalanced mass to the left wheel center in a downward direction with a force of 0.8 N (Table 8), referring to the relevant literature [8]. The SVSA angles obtained through the roll analysis are presented in Table 9.

Table 8. Unbalanced mass condition.

Type	Direction	Value (N)
Linear	x-axis	0
	y-axis	0
	z-axis	−0.8

Table 9. SVSA angle in roll analysis based on SRS.

Type	Max(°)	Min(°)
Base	3.205	−3.549
Type 1	3.226	−3.566
Type 2	3.223	−3.564
Type 3	3.301	−3.447
Type 4	3.156	−3.502
Type 5	3.172	−3.518
Type 6	3.120	−3.467

Each configuration exceeded the initially set SVSA angle range. Under flat road conditions, all the configurations exhibited the same SVSA angle with a maximum of 3.389 deg and a minimum of −3.470 deg. However, different SVSA angles were observed for each case when the vertical displacements of the left and right wheel centers of the vehicle differed (Figure 9).

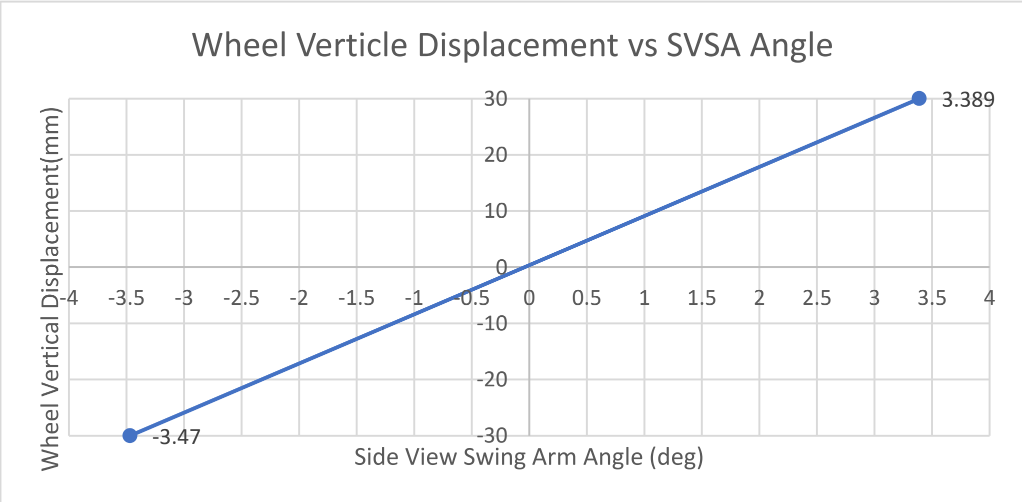

Figure 9. SVSA angle plot based on SRS.

Notably, in the roll analysis, the configurations with the convex curvature of the reinforcement beam (Type 1 to Type 3) had smaller negative SVSA angles than the baseline configuration, whereas configurations with concave curvature (Type 4 to Type 6) had larger negative SVSA angles than the baseline configuration. Among the seven types, Type 1 had the smallest SVSA angle, indicating the best driving stability according to the SRS criterion.

3.4. Driving Stability Analysis Based on Impact Hardness and Memory Shake

During everyday driving, vehicles encounter smooth roads and obstacles, such as speed bumps or gravel, resulting in excessive vibrations transmitted to the driver as impacts. The magnitude of these impacts on the driver was evaluated based on impact hardness and memory shake. Although a bump model was initially considered to simulate the impact, it was replaced with roll analysis, leveraging the vertical displacement of the wheels caused by road obstacles. The SVSA angle obtained from the ride and roll analysis are presented in Tables 10 and 11, respectively.

Figure 10 shows the process of analyzing the dynamic behavior of the left and right wheels. Through ride and roll analysis, the change in SVSA angle for each type was confirmed graphically (Figure 11) when the wheels on the left and right sides were shaken up and down up to 30 mm.

Table 10. SVSA angle in ride analysis based on impact hardness and memory shake.

Type	Max(°)	Min(°)
Base	3.547	−3.672
Type 1	3.536	−3.673
Type 2	3.536	−3.673
Type 3	3.536	−3.673
Type 4	3.536	−3.673
Type 5	3.536	−3.673
Type 6	3.536	−3.673

Table 11. SVSA angle in roll analysis based on impact hardness and memory shake.

Type	Max(°)	Min(°)
Base	3.306	−3.443
Type 1	3.258	−3.397
Type 2	3.273	−3.412
Type 3	3.281	−3.419
Type 4	3.250	−3.461
Type 5	3.222	−3.458
Type 6	3.320	−3.456

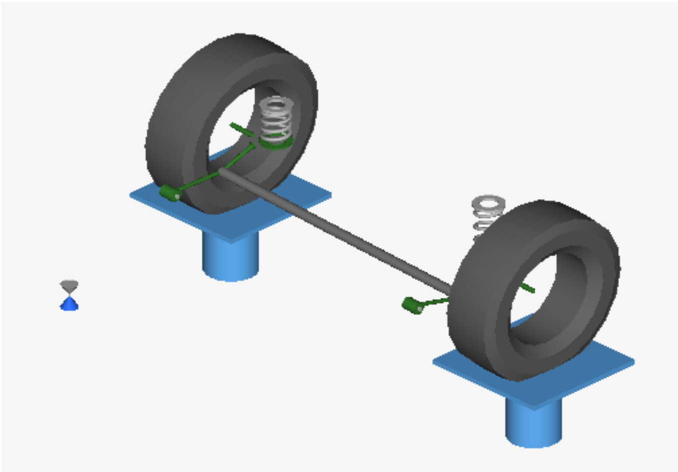

Figure 10. Rolling situation.

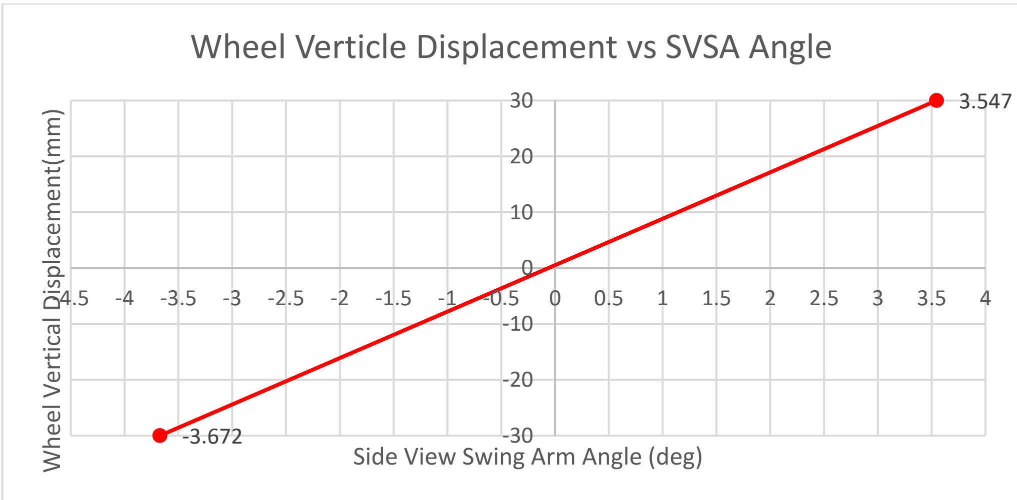

Figure 11. SVSA angle plot based on impact hardness and memory shake.

Each of the seven types of torsion beams exceeded the initially set SVSA angle range, and all types, except Base, showed the same SVSA angle when driving on a flat road, but there was no significant difference from the base SVSA angle. When the vertical displacement of the center of the left and right wheels of the vehicle was reserved, different values were shown for each type.

In the roll analysis, the configurations with the convex curvature of the reinforcement beam (Type 1 to Type 3) had a negative SVSA angle larger than Base while configurations with concave curvature (Type 4 to Type 6) showed a smaller negative SVSA angle than Base. Among the seven types, the smallest SVSA angle was measured in Type 4. Thus, based on the impact hardness and memory shake factors, Type 4 offers the best driving stability.

3.5. Comprehensive Driving Stability Analysis

Based on the above analysis, summarized in Tables 12 and 13, the Type 1 and Type 4 configurations were found to exhibit superior driving stability in terms of SRS, impact hardness, and memory shake. Because the ride and roll analysis used in the driving stability evaluation was static, it was not possible to represent the acceleration at specific positions [8]. The final configuration was determined by considering the following four aspects:

1. Higher positive SVSA angles lead to a decrease in memory shake performance.
2. Dramatic differences in driving stability may be less noticeable for short driving distances.
3. Taking into account the drivers' perception of lateral swaying may be more dramatic in cornering situations.
4. Even if the difference in SVSA angle is small, a difference in SVSA length may occur depending on the specifications of the vehicle to which the cross-member of the torsion beam suspension will be applied, which may ultimately result in a difference in tire wheel displacement.

Table 12. Best SVSA angle in ride analysis.

Evaluation Factor	Type	Max(°)	Min(°)
Smooth Road Shake	Type 1	3.389	−3.740
	Type 4	3.389	−3.740
Impact Hardness and Road Shake	Type 1	3.536	−3.673
	Type 4	3.536	−3.673

Table 13. Best SVSA angle in roll analysis.

Evaluation Factor	Type	Max(°)	Min(°)
Smooth Road Shake	Type 1	3.226	−3.566
	Type 4	3.156	−3.502
Impact Hardness and Road Shake	Type 1	3.258	−3.397
	Type 4	3.250	−3.461

According to Lee et al. [8], SRS sensitivity response characteristics can be improved as the SVSA angle decreases, and it was analyzed that the SRS sensitivity was 95% when the SVSA angle was −3 degrees. In this study, Type 4 is analyzed to have an SRS sensitivity of 94.16%. Also, we believe that Type 4 will be better at improving driving stability than Type 1. Considering these four aspects, the Type 4 configuration was identified as the most favorable option for overall driving stability among the cross-sections of the torsion beam used in this study.

4. Conclusions

The torsion beam suspension in vehicles is known to exhibit significant responses, even to small vibrations, and is difficult to adjust, unlike in independent suspension systems. Because of these drawbacks, the torsion beam suspension provides poor ride comfort. In this study, to enhance the structural stability of the rear torsion beam suspension in small SUVs, various shapes of cross-members with additional reinforcements were investigated, and structural and stiffness analyses were performed. Driving stability analyses were conducted for cross-member shapes with different reinforcement curvatures, and the following conclusions were drawn:

(1) To achieve structural stability in a torsional beam, it is crucial to minimize both bending and torsional stresses. This study revealed that the reinforcements with concave shapes exhibited lower stresses than those with convex shapes.

(2) As the torsional rigidity increased, torsional deformation caused by the external forces decreased, indicating stronger stiffness. The analysis results showed that,

among the concave shapes, Type 4, with higher torsional rigidity, exhibited the most stable structure.

(3) Based on a multibody dynamics simulation, the SVSA angle data for different cross-member shapes were analyzed, and the results showed that the Type 4 shape provided the most stable ride. Although comfort perception based on the driving habits of the drivers may differ significantly, adopting a Type 4 cross-member shape could lead to noticeable overall improvements in driving stability.

(4) SRS, impact hardness, and memory shake represent the longitudinal and vertical accelerations experienced by the driver at the steering wheel, seat, and foot positions, respectively, during vehicle operation. Based on the analysis results, Types 1 and 4 exhibited the most comfortable ride characteristics for each of these factors.

Generally, ride comfort evaluation is performed based on the vibration caused by acceleration under dynamic conditions. In contrast, the analysis in this study was based on the geometry factor called SVSA under static conditions, because SVSA is a kinematic factor and does not perform equally well under dynamic conditions.

Author Contributions: K.C., Y.L. and J.L. conceived and designed the data analysis, analyzed the data, and wrote the paper; K.C. and Y.L. performed the analysis and produced the analytic data; J.L. researched the paper and proposed the direction. All authors have read and agreed to the published version of the manuscript.

Funding: This research received no external funding.

Institutional Review Board Statement: Ethical review and approval are not applicable for this study as it does not involve humans or animals.

Informed Consent Statement: Informed consent was obtained from all subjects involved in the study.

Data Availability Statement: The data presented in this study are available on request from the corresponding author.

Acknowledgments: This study was supported by Soongsil University, Republic of Korea.

Conflicts of Interest: The authors declare no conflict of interest.

References

1. Hyundai. "Hyundai's Sales Record Data", Last Modified May 2023. Available online: https://www.hyundai.com/kr/ko/ir-information/sales/sales-record (accessed on 1 October 2023).
2. Kang, J. Kinematic Analysis of Torsion Beam Rear Suspension. *Trans. Korea Soc. Automot. Eng.* **2004**, *12*, 146–153.
3. Kang, J. A Study on Structual Design of Torsion Beam Rear Suspension. *Trans. Korea Soc. Automot. Eng.* **2005**, *13*, 146–153.
4. Kim, B.C.; Park, Y.W.; An, S.H.; Lim, D.M. Torsion Beam Shape Optimization Using Design of Experiment. *Trans. Korea Soc. Automot. Eng.* **2011**, *2011*, 924–928.
5. Jang, J.; Kim, Y.; Na, S.; Heo, J. Optimization for Tubular Torsion Beam Using Hot Stamping Method. In Proceedings of the Autumn Conference Papers of Korea Society of Automotive Engineers, Daejeon, Republic of Korea, 19 November 2008; pp. 231–232.
6. Lee, K.; Joo, H.; Kim, J.; Park, C.; Go, H.; Ryu, K. A Study on Durability Performance for Torsion Bem Tube with High Strength Steel. *Trans. Korea Soc. Automot. Eng.* **2013**, *1*, 1600.
7. Choi, G.; Cho, J. A Convergence Study by Structural Analysis on Torsion Beam Suspension of Rear Wheel. *J. Korea Converg. Soc.* **2019**, *10*, 187–192.
8. Lee, J.; Choi, J. Analysis and Design Sensitivity Study for Improving Smooth Road Shake of a Vehicle with Torsion Beam Rear Suspension. In Proceedings of the Autumn Conference of Korea Society of Automotive Engineers, Goyang, Republic of Korea, 20 November 2013; Volume 1, pp. 530–535.
9. Zhang, B.; Wang, H.; Li, Z.; Zhou, R. Dynamic modeling of torsion bar spring suspension and sensitivity analysis of K&C characteristics. *J. Braz. Soc. Mech. Sci. Eng.* **2023**, *45*, 226.
10. Gao, J.; Han, P. Collaborative optimization of bushing installation angle and bushing stiffness of torsion beam suspension to improve the handing stability of the whole vehicle. *Adv. Mech. Eng.* **2022**, *14*, 16878132221101022. [CrossRef]
11. Ren, N.; Meng, Q.; Mei, J. Strength Analysis of Torsion Beam of a MPV vehicle Based on ADAMS. *J. Phys. Conf. Ser.* **2020**, *1634*, 012135. [CrossRef]
12. Wang, Y.X.; Ni, J.T.; Wang, A.G. Overall Strength Analysis of Trailing Arm Torsion Beam Suspension System. *IOP Conf. Ser. Mater. Sci. Eng.* **2018**, *422*, 012023. [CrossRef]

13. Jeong, T.; Lee, S.; Yim, H. Shape optimization of a torsion beam axle for improving vehicle handling performance. *Int. J. Autom. Technol.* **2017**, *18*, 813–822. [CrossRef]
14. Ramalingam, M.; Arun, K.T.; Jebaseelan, D.; Choi, S.B.; Jebaraj, C. Ride Comfort Analysis of Vehicle Seat Suspension Systems: A Co-Simulation Study. *SageJournals Noise Vib. Worldw.* **2023**. Available online: https://journals.sagepub.com/doi/10.1177/09574565231203246 (accessed on 1 October 2023).
15. Akbari, A. Improved Ride Comfort through High-Bandwidth Seat Control Coupled with Passenger Biomechanics Analysis. Ph.D. Thesis, UC DAVIS, Davis, CA, USA, 2023; pp. 1–117.
16. Banerjee, S.; Balamurugan, V.; Krishnakumar, R. Ride Comfort Analysis of Math Ride Dynamics Model of Full Tracked Vehicle with Trailing Arm Suspension. *Procedia Eng.* **2016**, *144*, 1110–1118. [CrossRef]
17. Hao, D.; Zhang, J.; Qiang, Y.; An, J.; Zhang, J. Vibration Comfort Evaluation of Child Safety Seat Based on Vehicle Ride Comfort. In Proceedings of the IEEE 3rd International Conference on Electronic Technology, Communication and Information, Changchun, China, 26–28 May 2023; pp. 1705–1713.
18. Koulocheris, D.; Vossou, C. Sensitivity Analysis of a Driver's Lumped Parameter Model in the Evaluation of Ride Comfort. *Vehicles* **2023**, *5*, 1030–1045. [CrossRef]
19. Kobayashi, H.; Kohriyama, M.; Nagata, M.; Ohashi, S. Study of Deceleration Control using the Power Regenerative Brake to Improve the Ride Comfort in the Electric Vehicle. In Proceedings of the 23rd International Conference on Electrical Machines and Systems, Hamamatsu, Japan, 24–27 November 2020; pp. 2046–2049.
20. Jung, K.; Kim, G.; Choi, J. Analysis and Design Sensitivity Study for Improving Impact hardness & Memory shake of a Vehicle with Torsion Beam Rear Suspension. In Proceedings of the Autumn Conference of Korea Society of Automotive Engineers, Yeosu, Republic of Korea, 18 November 2014; pp. 421–426.
21. Choi, S.; Han, S.; Park, J.; Jeon, K.; Choi, G.; Ko, H.; Lee, D. A Study on the simulation Model Verification for Performance Evaluation of Torsion Beam Axle. *Trans. Korea Soc. Automot. Eng.* **2004**, *2*, 623–629.
22. Hyundai. "Kona's Specifications", Last Modified March 2023. Available online: https://www.hyundai.com/kr/ko/e/vehicles/the-all-newkona/spec (accessed on 1 October 2023).